JCI The Journal of Clinical Investigation

β_1 Integrin/FAK/cortactin signaling is essential for human head and neck cancer resistance to radiotherapy

Iris Eke, … , Veit Sandfort, Nils Cordes

J Clin Invest. 2012;122(4):1529-1540. https://doi.org/10.1172/JCI61350.

Research Article Oncology

Integrin signaling critically contributes to the progression, growth, and therapy resistance of malignant tumors. Here, we show that targeting of β_1 integrins with inhibitory antibodies enhances the sensitivity to ionizing radiation and delays the growth of human head and neck squamous cell carcinoma cell lines in 3D cell culture and in xenografted mice. Mechanistically, dephosphorylation of focal adhesion kinase (FAK) upon inhibition of β_1 integrin resulted in dissociation of a FAK/cortactin protein complex. This, in turn, downregulated JNK signaling and induced cell rounding, leading to radiosensitization. Thus, these findings suggest that robust and selective pharmacological targeting of β_1 integrins may provide therapeutic benefit to overcome tumor cell resistance to radiotherapy.

β_1 Integrin/FAK/cortactin signaling is essential for human head and neck cancer resistance to radiotherapy

Iris Eke,[1] Yvonne Deuse,[1,2] Stephanie Hehlgans,[1,3] Kristin Gurtner,[2] Mechthild Krause,[1,2] Michael Baumann,[1,2] Anna Shevchenko,[4] Veit Sandfort,[1] and Nils Cordes[1,2]

[1]OncoRay — National Center for Radiation Research in Oncology and [2]Department of Radiation Oncology, Medical Faculty Carl Gustav Carus, Dresden University of Technology, Dresden, Germany. [3]Department of Radiotherapy and Oncology, University of Frankfurt, Frankfurt am Main, Germany. [4]Max Planck Institute of Molecular Cell Biology and Genetics, Dresden, Germany.

Integrin signaling critically contributes to the progression, growth, and therapy resistance of malignant tumors. Here, we show that targeting of β_1 integrins with inhibitory antibodies enhances the sensitivity to ionizing radiation and delays the growth of human head and neck squamous cell carcinoma cell lines in 3D cell culture and in xenografted mice. Mechanistically, dephosphorylation of focal adhesion kinase (FAK) upon inhibition of β_1 integrin resulted in dissociation of a FAK/cortactin protein complex. This, in turn, downregulated JNK signaling and induced cell rounding, leading to radiosensitization. Thus, these findings suggest that robust and selective pharmacological targeting of β_1 integrins may provide therapeutic benefit to overcome tumor cell resistance to radiotherapy.

Introduction

Resistance to radiotherapy and chemotherapy significantly aggravates tumor control and cure for patients with cancer. Aside from well-known genetic and epigenetic alterations, increasing evidence points to microenvironmental factors as substantial contributors to acquired or developed tumor cell therapy resistance (1–3). Current strategies to enhance tumor cell eradication use targeting of key prosurvival molecules, such as cytoplasmic and nuclear protein kinases and growth factor receptors (4–6). A combination of a targeted agent plus conventional radiotherapy seems to be even more potent, as demonstrated in patients with head and neck squamous cell carcinomas (HNSCCs). Targeting the epidermal growth factor receptor using inhibitory antibodies caused significant improvement of both locoregional tumor control and overall survival of patients with HNSCC (7). In addition to transmembrane growth factor receptors, recent studies provide evidence for integrins as potential cancer targets (8–12). Similar to other integrin receptors, β_1 integrins are overexpressed in various tumor entities, including HNSCCs (13, 14), and have been described as strong promoters of HNSCC development and tumorigenesis and essential determinants of tumor cell resistance to therapy (15).

Integrins are transmembrane cell surface receptors comprised of 18 α and 8 β subunits, which contribute to regulation of, e.g., cell survival, proliferation, invasion, and cancer therapy resistance (9, 16–20). While clinical trials evaluating β_1 integrin antagonist monotherapy (http://clinicaltrials.gov/ct2/results?term=integrin&pg=1) are still ongoing, targeting of β_1 integrin has demonstrated strong potential in preclinical studies to sensitize cancer cells to conventional radiotherapies and chemotherapies (16, 21, 22). However, the underlying molecular mechanisms of how β_1 integrins confer tumor cell radioresistance remain largely unclear.

Owing to a lack of intrinsic kinase activity of integrins, cytoplasmic signaling molecules and adapter proteins are recruited to cytoplasmic integrin tails for signaling and are highly likely to be critically involved in resistance mechanisms (23, 24). One of these essential mediators of integrin signals is focal adhesion kinase (FAK), which functions in cell motility, proliferation, and the cellular stress response to ionizing radiation and chemotherapy (25–27). FAK, a 125-kDa nonreceptor protein kinase, transmits signals from both integrins and growth factor receptors and is overexpressed and hyperphosphorylated in various cancers originating, e.g., from liver (28), breast (29), and head and neck (30). The kinase activity of FAK is regulated through Y397 autophosphorylation upon activation of β integrins or growth factor receptors (31). For full kinase activation, additional sites, such as Y576 and Y577 in the activation loop, are phosphorylated by Src family kinases. Subsequently, activated Src phosphorylates the Crk/p130Cas complex, paxillin at Y118 and Y31, and c-Jun NH_2-terminal kinase (JNK) (32). Intriguingly, phosphorylation of PAK and Rac1 by JNK1 could be connected to actin reorganization via cofilin-mediated F-actin severing (33). Although integrin-mediated cell adhesion and the β_1 integrin–FAK interplay have extensively been explored (24, 34), it remains elusive how FAK signals between β_1 integrin and regulators of the actin cytoskeleton such as cortactin for prosurvival signaling.

Cortactin is a multidomain adapter protein, essentially contributing to cortical actin regulation (35, 36). Regulation of this pool of actin is controlled by a variety of actin regulatory proteins at integrin or cadherin adhesion sites and is important in many normal and pathologic cell processes, such as adhesion, migration, morphogenesis and tumor progression, and metastasis (37, 38). Aside from formins and Ena/VASP proteins, cortactin functions in actin assembly via interaction with the actin-related protein-2/3 (Arp2/3) complex, which is dependent on Src-mediated phosphorylation of cortactin at amino acid residues at Y421, Y466, and Y482 (39). While Src connects cortactin to growth factor receptors and MAPK signaling (40), Rho family GTPases, such as Rac and Cdc42, as well as a FAK/Arp3 interaction render cortactin function possible in stress fiber assembly and formation of lamellipodia and filopodia downstream of integrin signaling (41, 42).

Conflict of interest: The authors have declared that no conflict of interest exists.
Citation for this article: *J Clin Invest.* 2012;122(4):1529–1540. doi:10.1172/JCI61350.

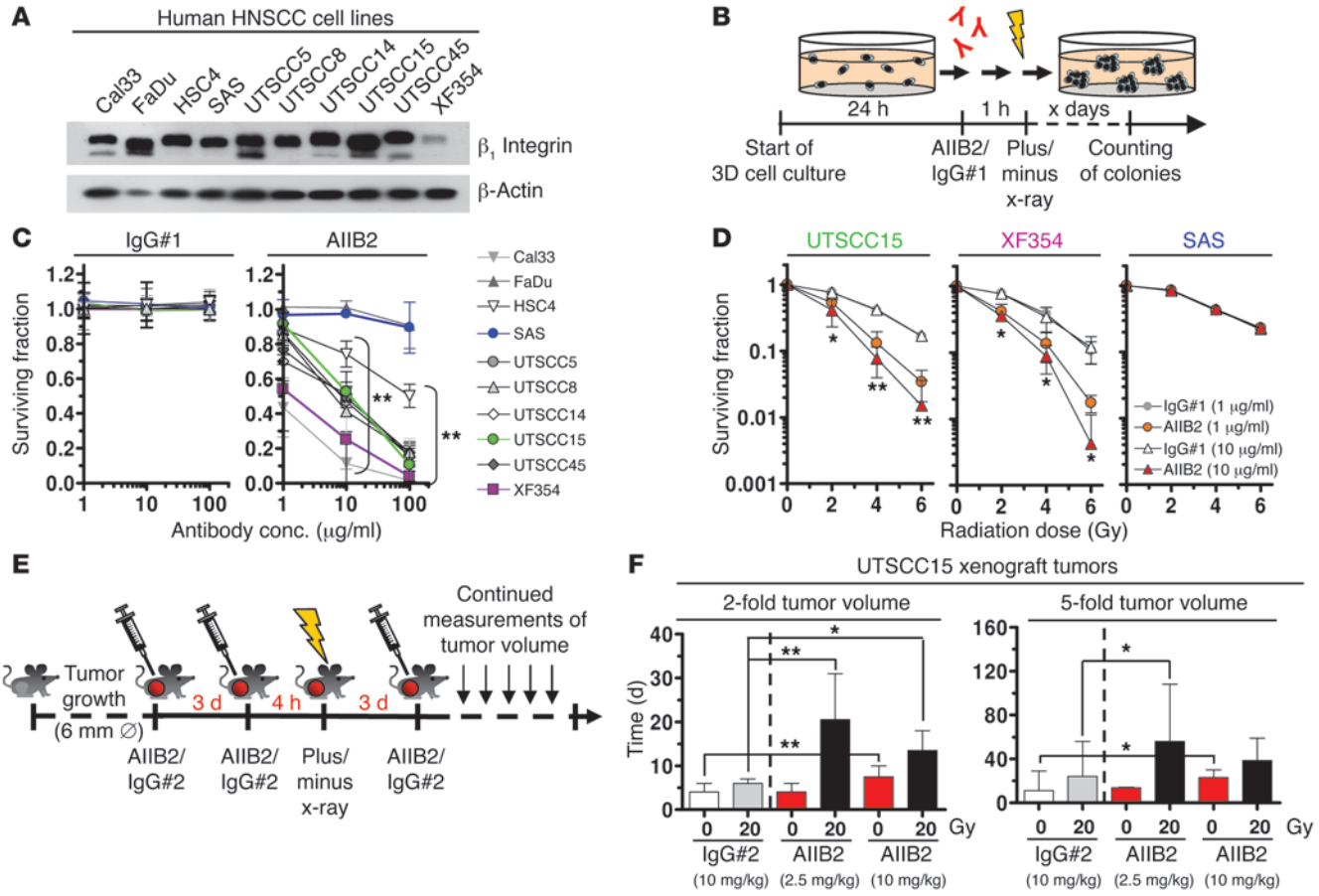

Figure 1

β_1 Integrin inhibition reduces HNSCC cell survival and confers radiosensitization in vitro and tumor growth delay in vivo. (**A**) Western blot analysis of β_1 integrin in HNSCC cell lines. β-Actin served as loading control. (**B**) Work flow of colony forming assay upon monoclonal inhibitory anti–β_1 integrin antibody (AIIB2) treatment of 3D lrECM cell cultures alone or combined with x-rays. (**C**) Clonogenic survival of 3D cell cultures upon AIIB2 administration (nonspecific IgG#1 as control) (mean ± SD; $n = 3$; *t* test; $^{**}P < 0.01$). conc., concentration. (**D**) Clonogenic radiation survival (0–6 Gy; mean ± SD; $n = 3$; *t* test; $^{*}P < 0.05$, $^{**}P < 0.01$) of 1-hour AIIB2 pretreated 3D lrECM cell cultures (nonspecific IgG#1 as control). (**E**) Experimental in vivo setup. Subcutaneous UTSCC15 tumors were grown in immunocompromised mice to a diameter of 6 mm. Mice received 3 antibody injections (day 0, 3, 6). Where indicated, 20 Gy x-ray radiation was applied 4 hours after second antibody injection. ∅, diameter. (**F**) Time to reach 2-fold and 5-fold tumor starting volume upon AIIB2 (or IgG#2 control) treatment is plotted against irradiation (medians ± 95% CI; $n = 10$–18; Mann-Whitney *U* test). Dashed lines separate IgG#2 control data from data of AIIB2 treatment. $^{*}P < 0.05$, $^{**}P < 0.01$. See also Supplemental Figures 1–11.

The goal of our study was to understand the first mechanistic steps of sensitization of tumor cells to ionizing radiation by β_1 integrin inhibition in 3D cell culture and in vivo models. Here, we show that cell rounding and radiosensitization upon β_1 integrin inhibition are controlled by a FAK/cortactin interaction and downstream signaling to JNK1.

Results

β_1 Integrin inhibition sensitizes 3D laminin-rich ECM HNSCC cell cultures to irradiation. To evaluate the clonogenic cell survival upon β_1 integrin inhibition, we first treated a panel of 10 human β_1 integrin–expressing HNSCC cell lines with an inhibitory anti–β_1 integrin mAb (i.e., AIIB2) (Figure 1, A–C, and Supplemental Figure 1, A–C; supplemental material available online with this article; doi:10.1172/JCI61350DS1). By using a 3D laminin-rich ECM–based (lrECM-based) cell culture model, which better mimics physiological growth conditions than 2D cultures, HNSCC cells showed AIIB2 concentration-dependent cytotoxicity relative to that of 2 different nonspecific IgG controls (Figure 1C and Supplemental Figure 1, B and C). Next, we assessed whether β_1 integrin inhibition modulates the cellular sensitivity to x-rays and found that AIIB2 enables radiosensitization in 8 out of 10 cell lines relative to cell lines treated with nonspecific IgG isotype antibody no. 1 (IgG#1) controls (Figure 1D and Supplemental Figure 2). Analysis of apoptosis in 3D UTSCC15 cell cultures revealed low (~8%) but significantly increased levels under combined AIIB2/irradiation treatment conditions (Supplemental Figure 3A), which was supported by enhanced caspase-3 cleavage (Supplemental Figure 3, B and C). Confirmatory data for clonogenic survival were generated in UTSCC15 cells with another inhibitory anti–β_1 integrin antibody, termed mAb13 (Supplemental Figure 4A), and in UTSCC15, XF354, and SAS cells using siRNA directed toward β_1 integrin (Supplemental Figure 4B). To exclude antibody-mediated side effects, we treated β_1 integrin knockdown cultures with AIIB2 and observed radiosensitization similar to that

detected with knockdown alone (Supplemental Figure 4C). Thus, these findings demonstrate an essential role of β_1 integrins for HNSCC cell survival upon radiation.

Targeting β_1 integrins causes significant growth delay of human HNSCC tumor xenografts. To evaluate the effect of β_1 integrin inhibition in vivo, we established xenografts from the responder UTSCC15 HNSCC cell line in immunocompromised nude mice for growth delay measurements (Figure 1, E and F). Grown tumors (~6-mm diameter) were treated with 3 cycles of AIIB2 (isotype IgG [IgG#2] as control) alone at day 0, 3, and 6 or with a combination of AIIB2 treatment and a single x-ray dose of 20 Gy 4 hours after the second AIIB2 i.p. injection (Figure 1E). Even in the absence of irradiation, a significant ($P < 0.01$) growth delay was achieved at a 10 mg/kg AIIB2 concentration as compared with IgG#2 controls (Figure 1F, Supplemental Figure 5, and Supplemental Tables 1 and 2). Designed as a pilot experiment, the combined AIIB2 administration and 20 Gy single x-ray dose resulted in a significant prolongation of the time to reach the 2-fold (2.5 mg/kg and 10 mg/kg, respectively) and 5-fold (2.5 mg/kg) starting tumor volume for the AIIB2 schedule relative to that for the irradiated IgG#2 control tumors (Figure 1F and Supplemental Figure 5). Except for differences in the rate of mitosis (Supplemental Figure 6), additional analyses of UTSCC15 tumor xenografts did not reveal treatment-related modifications of the proliferation markers BrdU and Ki-67 (Supplemental Figures 7 and 8), animal weight (Supplemental Figure 9), ratios of necrotic area to vital area and hypoxic area to vital area (Supplemental Figure 10), or signs of metastatic spread (Supplemental Figure 11).

Distinct modulation of FAK-associated signaling upon β_1 integrin inhibition. To identify the signaling network modifications that critically contribute to the enhanced radiosensitivity upon β_1 integrin targeting, we performed a phosphoproteome array analysis (Kinexus). AIIB2 treatment of 3D lrECM HNSCC cell cultures caused reduced phosphorylation of FAK, PKA, PKC, and JNK, while phosphorylation of PAK1/2/3, Src, GSK3α and GSK3β, GRK2, ERK2, and Raf1 was induced at specific sites (Figure 2A, Supplemental Figure 12 [unchanged protein kinases], and Supplemental Table 3). In line with a lack of FAK phosphorylation, we found reduced phosphorylation of FAK-associated proteins, paxillin, p130Cas, and JNK1, in both 3D lrECM UTSCC15 and XF354 cell cultures and UTSCC15 tumor xenografts (Figure 2B and Supplemental Figure 13, A and B). In contrast, the nonresponder cell line SAS showed stable phosphorylation of investigated proteins upon AIIB2 treatment (Figure 2B and Supplemental Figure 13, A and B). As β_1 integrin inhibition led to JNK2 dephosphorylation in both responder and nonresponder cell lines (Figure 2B and Supplemental Figure 13, A and B), we hypothesized that JNK2 is less relevant for β_1 integrin inhibition-dependent radiosensitization.

To evaluate a direct link between β_1 integrins and FAK as a putative proximal downstream target, we performed an in situ proximity ligation assay (PLA; Duolink), which allows the detection of single protein events, such as protein interactions, at an exact subcellular location (43). Indeed, upon AIIB2-mediated β_1 integrin inhibition, the direct β_1 integrin/FAK interaction was lost in UTSCC15 cells in contrast to that in SAS cells within 1 hour, indicated by strongly diminished subcellular interaction sites (Figure 2C, red dots).

FAK and JNK1 essentially contribute to radioresistance. To demonstrate that distinct members of the FAK downstream signaling pathway are responsible for the increased sensitivity to x-rays upon β_1 integrin inhibition, we performed single- and double-knockdown experiments of FAK, Src, JNK1, and JNK2, with or without AIIB2 treatment. Evidently, 3D clonogenic radiation survival was significantly and similarly reduced by single FAK or JNK1 and double FAK/JNK1 knockdown in both responder cell lines, UTSCC15 and XF354, suggesting that these molecules function in the same signaling pathway (Figure 2D). As the depletion of these protein kinases also diminished the radiation survival of the nonresponder cell line SAS, although to a lesser extent, FAK and JNK1 obviously have further tasks aside from integrin signaling. Depletion of Src and JNK2 did not affect clonogenic radiation survival (Supplemental Figure 14). To test whether FAK and JNK1 are critical to AIIB2-mediated radiosensitization, we combined FAK and JNK1 knockdown with AIIB2 treatment and found radiosensitivity similar to that observed for knockdown alone (Figure 2E). From these observations, we conclude that the enhanced sensitivity to x-rays by β_1 integrin inhibition in 3D lrECM–grown HNSCC cells results from the deactivation of a signaling pathway involving FAK and JNK1.

FAK determines the effectiveness of β_1 integrin inhibition on radiosensitization. To provide more evidence that FAK contributes to radioresistance and is the key upstream determinant of the enhanced sensitivity to x-rays upon β_1 integrin inhibition, we stably transfected the responder cell line UTSCC15 with plasmids encoding for wild-type FAK-GFP (FAKwt-GFP), constitutively active FAK-GFP (FAKca-GFP; K→E plus K→E at residues 578 and 581 [K578E/K581E]) (44), and GFP empty vector control (Figure 3, A and B). Intriguingly, FAKca-GFP transfectants were completely insensitive to AIIB2 as compared with FAKwt-GFP cells, which showed reduced AIIB2 sensitivity, and GFP controls, which reacted like parental cells (Figure 3C). These data were in line with a stable FAK/β_1 integrin interaction (Figure 3D) and a stable localization of FAK Y397 phosphorylation to focal adhesions (FAs) (Supplemental Figure 15) in FAKca-GFP but not FAKwt-GFP or GFP transfectants, as analyzed with in situ PLA technology or indirect immunofluorescence, respectively.

Next, we assessed the clonogenic radiation survival of the transfectant cell lines and made the following observations. First, the intrinsic radiosensitivity was markedly reduced in FAKwt-GFP cells and even further reduced in FAKca-GFP cells relative to that in GFP controls (Figure 3E). Second, the AIIB2-related radiosensitization was completely abolished by exogenous expression of FAKca-GFP cells in contrast to a remaining concentration-dependent AIIB2 susceptibility in FAKwt-GFP and GFP cells (Figure 3E). From these observations, we conclude that the stability of the β_1 integrin/FAK interaction is one of the key events controlling radiosensitization of 3D lrECM–grown HNSCC cells.

Susceptibility to β_1 integrin inhibition determines FA disassembly and cortactin dissociation from FAK. As cell rounding and FA disassembly upon integrin inhibition have been shown previously but have not yet been investigated in the context of tumor cell radiosensitivity, we monitored responder UTSCC15 cells and nonresponder SAS cells. Intriguingly, cell rounding was observable in AIIB2-treated UTSCC15 cells (Figure 4A and Supplemental Videos 1 and 2) but not in SAS cells (Figure 4A and Supplemental Videos 3 and 4). Rounding was accompanied by FA disassembly and visualized by paxillin removal from FAs in stably transfected paxillin-GFP–expressing UTSCC15 cells (Supplemental Figure 16 and Supplemental Videos 5 and 6). From these findings, we hypothesized that enhanced radiosensitivity upon AIIB2-mediated β_1 integrin blocking in UTSCC15 cells, but not SAS cells, was a consequence of FA disassembly and actin remodeling.

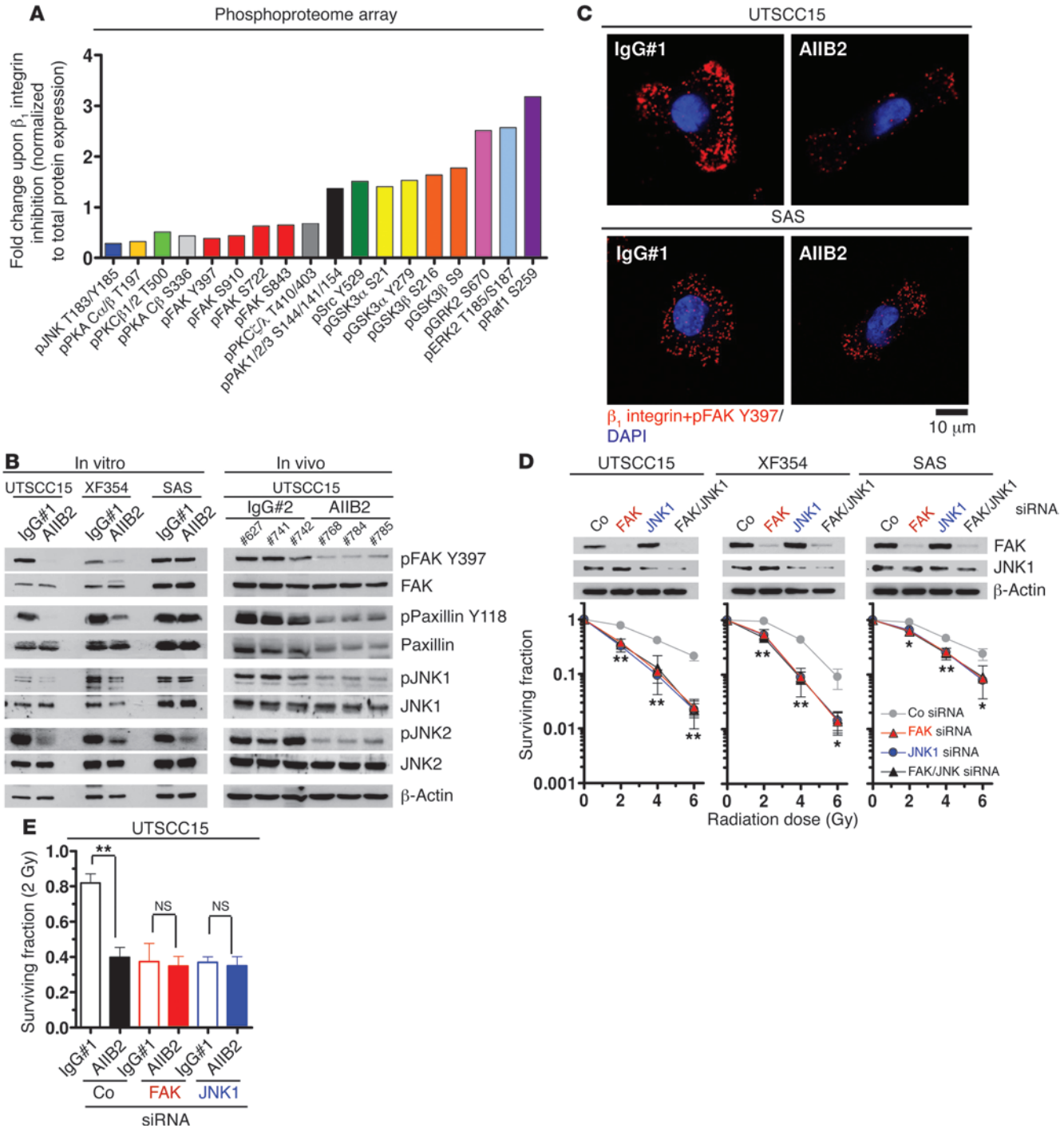

Figure 2

Perturbed FAK/JNK1 signaling by β_1 integrin inhibition causes tumor cell radiosensitization. (**A**) Phosphoproteome array-based analysis on whole cell lysates of 3D UTSCC15 cell cultures treated for 1 hour with AIIB2 (IgG#1 as control) is plotted as fold change after normalization to total protein expression (complete list in Supplemental Table 3). (**B**) Western blotting on protein lysates from AIIB2-treated 3D cell cultures and UTSCC15 tumor xenografts ($n = 3$). Numbers indicate animal numbers. (**C**) PLA using anti–β_1 integrin and anti–FAK Y397 antibodies and confocal microscopy on AIIB2-treated (100 μg/ml; 1 hour) cells (IgG#1 as control). DAPI was used for nuclear staining. Scale bar: 10 μm. (**D**) Clonogenic radiation survival of FAK or JNK1 or FAK/JNK1 double knockdown. Data show mean ± SD ($n = 3$; t test; $^*P < 0.05$, $^{**}P < 0.01$). Co, nonspecific siRNA control. (**E**) Clonogenic radiation survival of FAK or JNK1 depleted cells, with or without AIIB2 treatment (100 μg/ml, 1 hour) and irradiation with 2 Gy (mean ± SD; $n = 3$; t test; $^{**}P < 0.01$). See also Supplemental Figures 1–14.

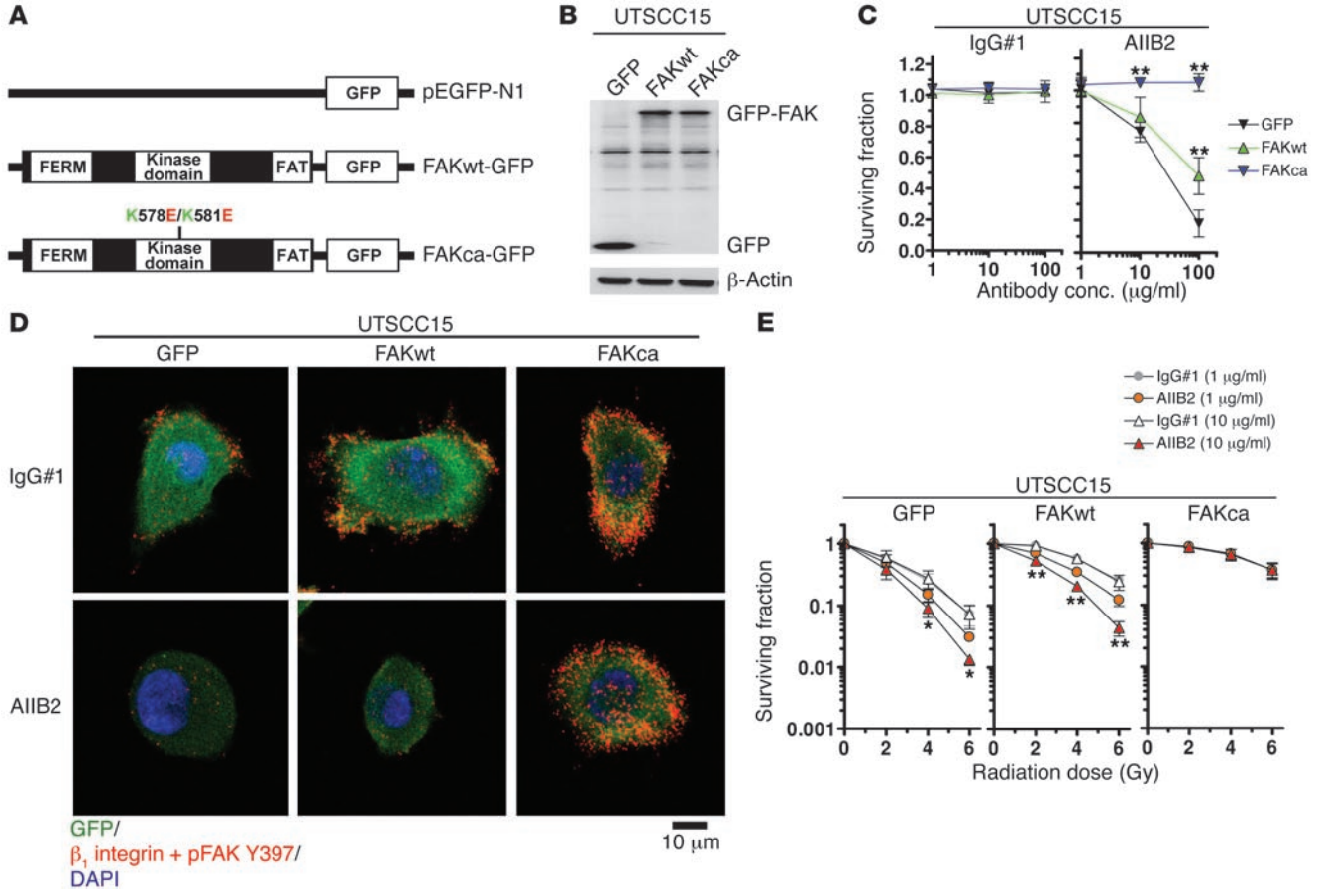

Figure 3

FAK-cortactin dispersion is essential for cell rounding and enhanced radiosensitivity. (**A**) Scheme of FAKwt-GFP, FAKca-GFP (K→E plus K→E at residues 578 and 581 [K578E/K581E]), and GFP empty vector controls (pEGFP-N1). (**B**) Western blot from whole cell lysates of UTSCC15 cells stably transfected with FAK-GFP fusion constructs indicated in **A**. β-Actin served as loading control. (**C**) Clonogenic survival of AIIB2-treated FAKca-GFP, FAKwt-GFP, and GFP transfectants (IgG#1 as control). Results show mean ± SD (n = 3; t test; $^{**}P < 0.01$). (**D**) PLA using anti–β_1 integrin and anti–FAK Y397 antibodies and confocal microscopy on AIIB2-treated UTSCC15 transfectants. DAPI was used for nuclear staining. Scale bar: 10 μm. (**E**) Clonogenic radiation survival of AIIB2-pretreated and irradiated (2–6 Gy) FAKca-GFP, FAKwt-GFP, and GFP transfectants. Results show mean ± SD (n = 3; t test; $^{*}P < 0.05$; $^{**}P < 0.01$). See also Supplemental Figure 15.

To connect FAK with the fast actin remodeling dynamics resulting from FA disassembly, we focused on the actin organization regulators cortactin, cofilin and moesin/ezrin, which have been identified to interact with FAK via immunoprecipitation and mass spectrometry (Supplemental Table 4). After AIIB2 treatment, cortactin phosphorylation at Y421 was suppressed, while other examined proteins remained unchanged (Figure 4B and Supplemental Figure 17). In situ PLA technology visualized a dissociation of cortactin from FAK, suggesting a physical link between these proteins (Figure 4C). Western blot analysis of FAK immunoprecipitates showed cortactin binding to FAK and cortactin release from FAK after AIIB2-dependent β_1 integrin inhibition to last at least 24 hours (Supplemental Figure 18) as compared with that in controls treated with either nonspecific IgG#1 or the stimulatory anti–β_1 integrin antibody TS2/16 (Figure 4D and Supplemental Figure 19A). Moreover, unlike FAKwt-GFP, FAKca-GFP maintained the cortactin interaction upon AIIB2-mediated β_1 integrin inhibition, as observed in GFP immunoprecipitates from whole cell lysates (Figure 4E and Supplemental Figure 19, B and C). These data identified cortactin as a downstream target of β_1 integrin/FAK signaling in 3D lrECM HNSCC cell cultures.

FAK/cortactin/JNK1 signaling regulates radiation cell survival. To verify the importance of the FAK/cortactin signaling pathway for radiosensitivity, 3D clonogenic radiation survival of UTSCC15, XF354, and SAS cells was measured after FAK knockdown, cortactin knockdown, or combined FAK/cortactin knockdown. Interestingly, cortactin knockdown alone resulted in a radiosensitization that was less pronounced relative to that of single FAK knockdown (Figure 5A), while radiation survival of FAK/cortactin double-knockdown cultures was the same as that in cultures after FAK knockdown (Figure 5A). On the basis of unchanged β_1 integrin levels in FAK knockdown cells (Supplemental Figure 20), our hypothesis is that FAK, due to its upstream positioning in the FAK/cortactin signaling pathway, mediates additional prosurvival, radiosensitivity-regulating signals aside from cortactin. The importance of the FAK/cortactin/JNK1 signaling pathway became clearer by treating the FAK, Src, JNK1, JNK2, or cortactin knockdown cell cultures with the clinically relevant dose per fraction of 2 Gy in the presence or absence of β_1 integrin inhibition by AIIB2. Strikingly, we only observed a loss of AIIB2-mediated radiosensitization upon depletion of

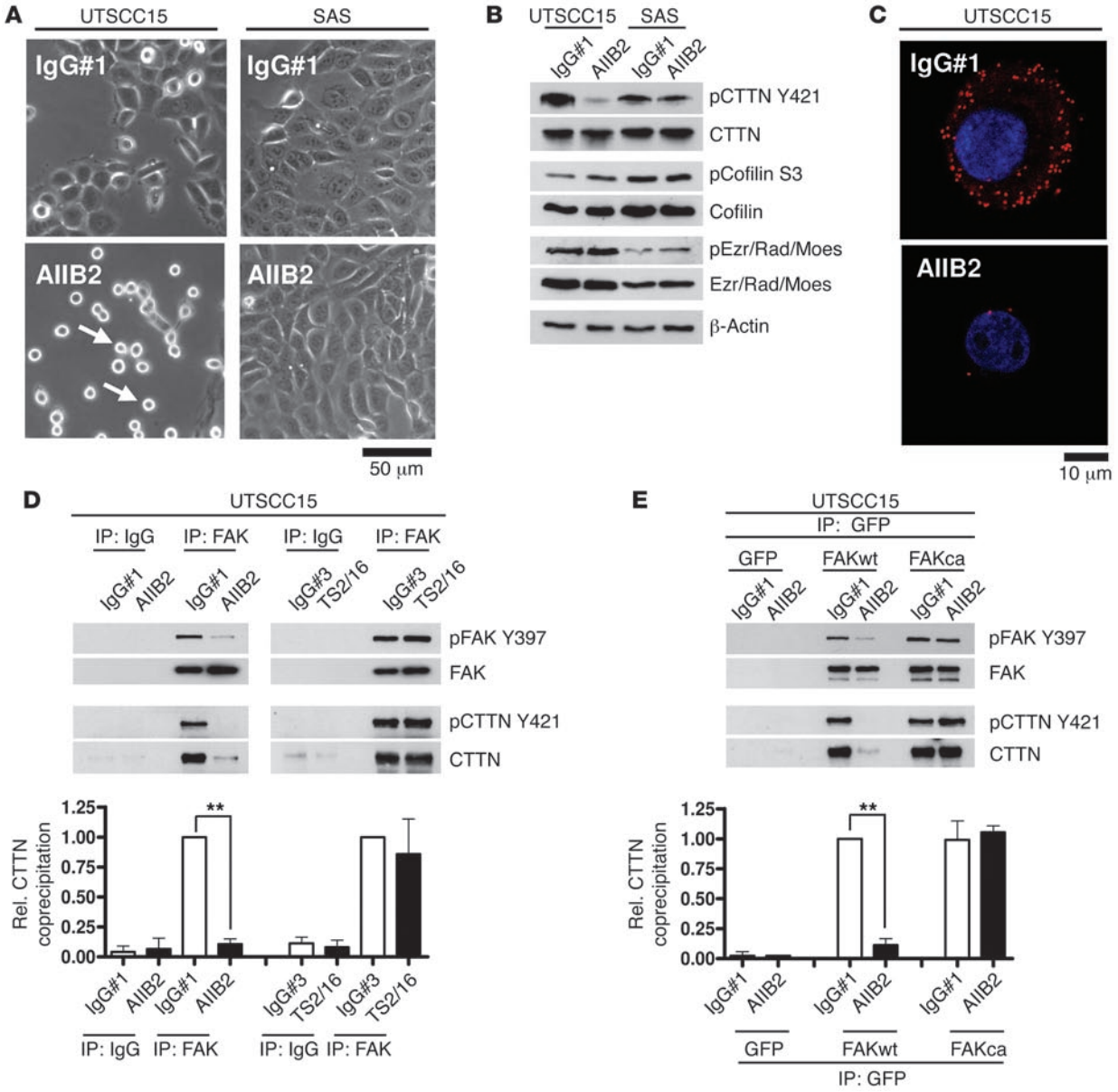

Figure 4

Disassembly of FAK/cortactin interaction upon β_1 integrin inhibition. (**A**) Phase-contrast microscopy for cell rounding (arrows) upon AIIB2-mediated β_1 integrin inhibition (IgG#1 as control). Scale bar: 10 μm. (**B**) Time course Western blot analysis on protein lysates from AIIB2-treated 3D cell cultures (n = 3). β-Actin served as loading control. Ezr/Rad/Moes, ezrin/radixin/moesin. (**C**) PLA using anti–β_1 integrin FAK and anti-CTTN antibodies and confocal microscopy on AIIB2-treated cells. DAPI was used for nuclear staining. Scale bar: 10 μm. (**D**) Western blot analysis of FAK and CTTN expression and phosphorylation of FAK immunoprecipitates. FAK immunoprecipitation was done from whole cell lysates of cells treated with AIIB2 or TS2/16 (a β_1 integrin–stimulating antibody). IgG#1 and IgG#3 served as controls. Results show mean ± SD (n = 3; t test; $^{**}P < 0.01$). Rel, relative; coprecipitation, coimmunoprecipitation. (**E**) Western blot analysis of FAK and CTTN expression and phosphorylation of GFP immunoprecipitates. GFP immunoprecipitation was done from whole cell lysates of AIIB2-treated FAKca-GFP, FAKwt-GFP, and GFP transfectants. IgG#1 served as control. Data show mean ± SD (n = 3; t test; $^{**}P < 0.01$). See also Supplemental Figures 16–19.

FAK, JNK1, and cortactin, indicating a specific signaling function downstream of β_1 integrins in HNSCC cells (Figure 2E and Figure 5B). In contrast, knockdown of Src and JNK2 failed to abrogate AIIB2-dependent radiosensitization compared with that in IgG#1 controls (Supplemental Figure 21).

In parallel, we evaluated the signaling hierarchy of FAK, cortactin, and JNK1 upon β_1 integrin blocking in whole cell lysates under diverse knockdown conditions. As shown in Figure 4B, AIIB2 caused a dephosphorylation of FAK Y397, JNK1 T183/Y185, JNK2 T183/Y185, and cortactin Y421 in 3D lrECM siRNA control cultures relative to IgG#1-treated siRNA control cultures (Figure 5, C and D, and Supplemental Figure 22, lane 1 and 2). FAK silencing translated into a lack of phosphorylation of all other investigated proteins, i.e., Src, JNK1, JNK2, cortactin. This

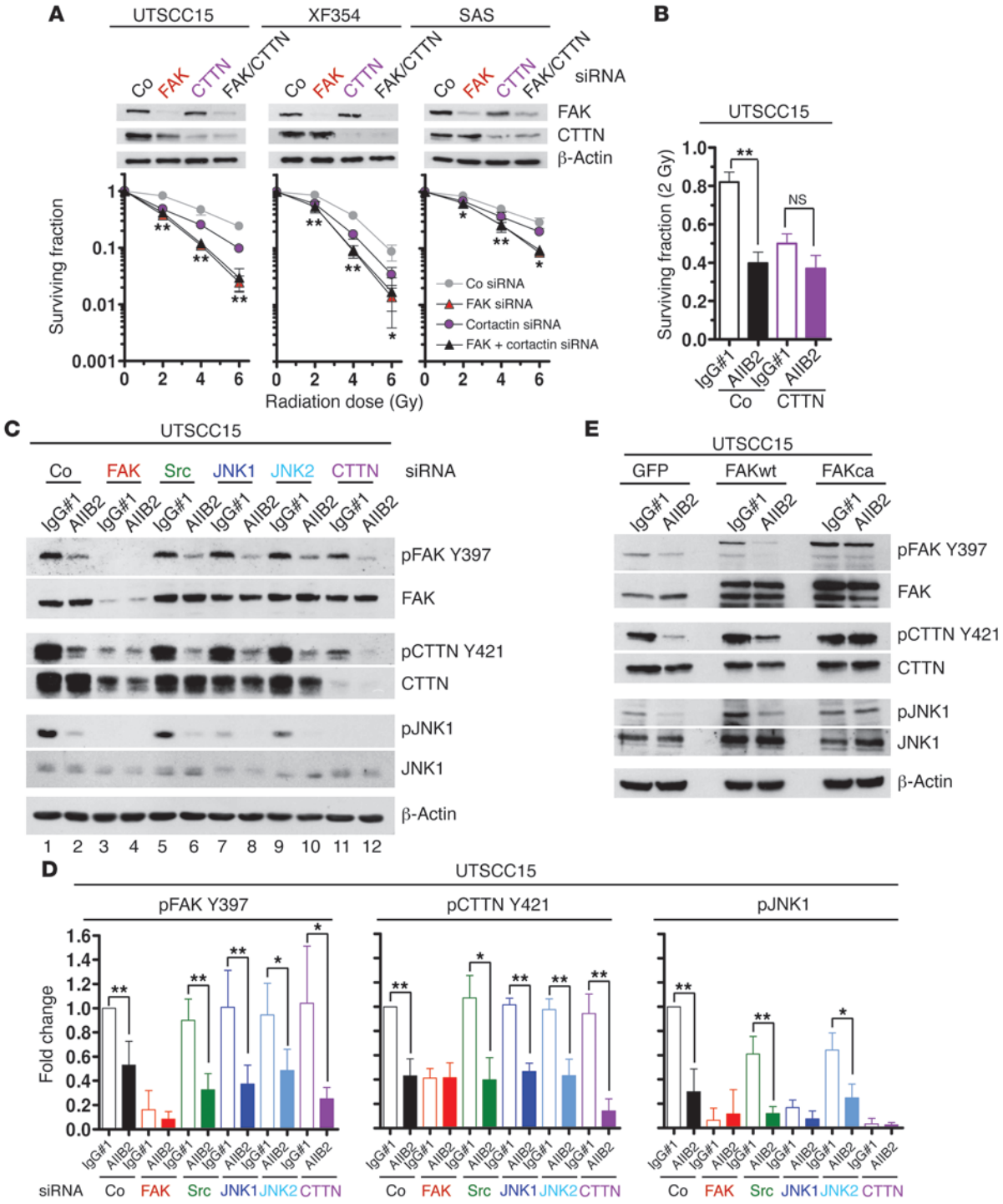

Figure 5

Cortactin in HNSCC radiation cell survival and β_1 integrin downstream signaling. (**A**) Clonogenic radiation survival of FAK and CTTN single- and double-knockdown 3D cell cultures (mean ± SD; $n = 3$; t test; $^*P < 0.05$; $^{**}P < 0.01$). (**B**) Clonogenic radiation survival of CTTN-depleted cells exposed to AIIB2 and 2 Gy (mean ± SD; $n = 3$; t test; $^{**}P < 0.01$). (**C**) Western blot analysis on indicated proteins from whole cell lysates of 3D UTSCC15 knockdown cell cultures. Subsequent to single knockdown of FAK, Src, JNK1, JNK2, or cortactin, cells were treated with AIIB2 (or IgG#1 as control) for 1 hour. β-Actin served as loading control. (**D**) Densitometric analysis of protein bands and protein phosphorylation shown in **C**. Results show mean ± SD ($n = 3$; t test; $^*P < 0.05$; $^{**}P < 0.01$). (**E**) Western blot analysis of FAK, CTTN, and JNK1 from whole cell lysates of AIIB2-treated FAKca-GFP, FAKwt-GFP, and GFP transfectants grown in 3D (IgG#1 as control). β-Actin served as loading control. See also Supplemental Figures 20–23.

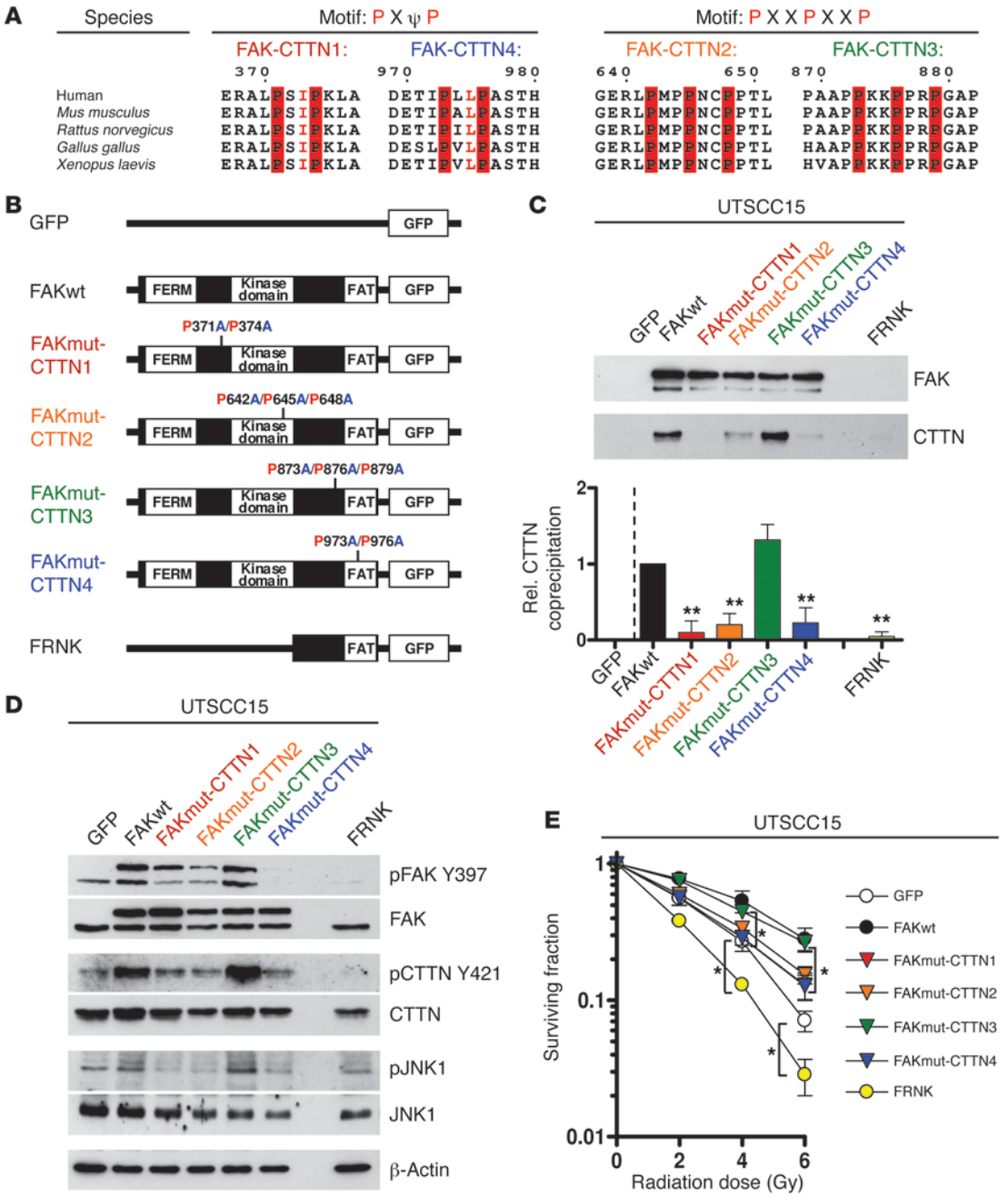

Figure 6

FAK interacts with cortactin to regulate cellular radiosensitivity. (**A**) FAK sequence homology search for putative cortactin binding sequences consisting of PXΨP or PXXPXXP. Numbers indicate amino acids. (**B**) Scheme of different FAK mutations (FAKmut-CTTN1–FAKmut-CTTN4) at putative cortactin binding sites using site-directed mutagenesis as well as FRNK cloned in pEGFP-N1 vector. (**C**) Cortactin binding efficacy in cells stably transfected with FAK-GFP plasmids expressing FAKwt, FAKmut-CTTN1 (P371A/P374A), FAKmut-CTTN2 (P642A/P645A/P648A), FAKmut-CTTN3 (P873A/P876A/P879A), or FAKmut-CTTN4 (P973A/P976A) or FRNK. Cells grew under 3D lrECM conditions. Data are mean ± SD. ($n = 3$; $^{**}P < 0.01$; *t* test). (**D**) Western blot evaluation of indicated proteins from whole cell lysates of diverse mutant 3D lrECM–grown FAK-GFP transfectants. (**E**) Clonogenic radiation survival (0–6 Gy x-rays) measured in 3D lrECM UTSCC15 cell cultures expressing the different cortactin binding mutations in FAK (FAKmut-CTTN1–FAKmut-CTTN4), FAKwt, FRNK, or GFP empty vector control. Data are mean ± SD. ($n = 3$; $^{*}P < 0.05$, *t* test). See also Supplemental Figure 24.

prevented further dephosphorylation by AIIB2 (Figure 5, C and D, lanes 3 and 4). Thus, FAK appears to function at the top of the examined signaling hierarchy, leading to deactivation of Src, JNK1, JNK2, and cortactin. Src, however, seemed to be located downstream of FAK and cortactin, because its knockdown affected neither phosphorylation of FAK nor the putative Src phosphorylation site Y421 of cortactin and allowed for FAK and cortactin downregulation by AIIB2 (Figure 5, C and D, lanes 5 and 6,

and Supplemental Figure 22). As JNK1 knockdown provided similar results, Src and JNK1 seemed to be located at the same position in the signaling pathway. Downstream of FAK and cortactin, JNK2 seemed to participate in JNK1 T183/Y185 and Src Y416 regulation (Figure 5, C and D, lanes 9 and 10 and Supplemental Figure 22). Depletion of cortactin had no impact on FAK phosphorylation (Figure 5, C and D, lanes 11 and 12). Due to their position downstream of cortactin, JNK1 and JNK2 phosphorylation was reduced when cortactin was depleted (Figure 5, C and D, and Supplemental Figure 22, lanes 11 and 12).

Using FAK transfectants, we show that a stable FAK/cortactin interaction in FAKca-GFP cells enables continuous JNK1 phosphorylation after AIIB2 treatment relative to that in FAKwt-GFP and GFP cells (Figure 5E and Supplemental Figure 23). These findings show that HNSCC cell sensitization to x-rays by β_1 integrin inhibition relies on a specific signaling cascade involving FAK, cortactin, and JNK1.

Proper FAK-cortactin binding controls cell survival after irradiation. In an attempt to identify a direct interaction between FAK and cortactin, FAK was probed for putative cortactin binding domains consisting of PXΨP or PXXPXXP sequences using a homology search (45), and we found 4 of these SH3 consensus binding motifs in FAK (Figure 6A). Using site-directed mutagenesis, either 2 (FAKmut–cortactin 1 [FAKmut-CTTN1], P→A at residues 371 and 374 [P371A/P374A]; FAKmut-CTTN4, P→A at residues 973 and 976 [P973A/P976A]) or 3 (FAKmut-CTTN2, P→A at residues 642, 645, and 648 [P642A/P645A/P648A]; FAKmut-CTTN3, P→A at residues 873, 876, and 879 [P873A/P876A/P879A]) proline residues were mutated to alanine (Figure 6B). These constructs, and, additionally, FAK-related non-kinase (FRNK; Figure 6B) as a control, were fused to GFP and stably expressed in UTSCC15 cells (Figure 6D). GFP immunoprecipitation from whole cell lysates demonstrated 3 loss-of-binding mutations in FAK compared with FAKwt (Figure 6C and Supplemental Figure 24, A and B). The first one localized at the first linker domain connecting the four-point-one, ezrin, radixin, moesin (FERM) and kinase domains (i.e., P371A/P374A), the second localized at the kinase domain (i.e., P642A/P645A/P648A), and the third localized at the FAT domain (C-terminal focal-adhesion targeting; i.e., P973A/P976A) (46). The fourth mutation, at the putative binding motif located at the C-terminal end of the second linker domain (P873A/P876A/P879A), had no effect on cortactin binding (Figure 6C). The absence of cortactin in FRNK-expressing cells suggests dependency of FAK/cortactin interactions on FAK activity (Figure 6C), a hypothesis supported by the fact that the FERM and kinase domains cooperatively serve in FAK kinase activity regulation (42), while the FAT domain promotes FAK localization to cytoplasmic integrin tails (46).

Since cortactin releases from unphosphorylated FAK upon β_1 integrin deactivation, we subsequently analyzed whether the mutated PXΨP or PXXPXXP binding sequences compromise FAK activity. Intriguingly, the distinct PXΨP and PXXPXXP mutations in the FERM-kinase linker, kinase, and FAT domains as well as FRNK expression significantly ($P < 0.05$) reduced FAK Y397 autophosphorylation relative to that in FAKwt and FAKmut-CTTN3 (Figure 6D and Supplemental Figure 24C). Whether these mutations affect downstream signaling to cortactin and JNK1 and eventually translate into altered radiosensitivity was examined next. We found strongly diminished cortactin and JNK1 phosphorylation in the different FAK mutants, which paralleled modifications in FAK Y397 phosphorylation (Figure 6D and Supplemental Figure 24C).

Most importantly, cells expressing the loss-of-binding mutations (i.e., FAKmut-CTTN1, FAKmut-CTTN2, FAKmut-CTTN4) or FRNK showed significantly ($P < 0.05$) enhanced radiosensitivity as compared with cells expressing mutations in the kinase-FAT linker (i.e., FAKmut-CTTN3) or FAKwt (Figure 6E and Supplemental Figure 24D). These results clearly show that FAK and cortactin interact and that functional cortactin binding motifs on FAK are placed within those domains essentially involved in the regulation of FAK kinase activity. Cortactin binding to FAK depends on the FAK activity status. Moreover, these findings provide evidence for prosurvival and radioresistance-mediating signals via a β_1 integrin/FAK/cortactin/JNK1 axis.

Discussion

Therapy resistance mechanisms in human cancers are determined by intracellular factors and interactions of cells with ECM or neighboring cells as well as the tumor microenvironment. While integrin cell adhesion receptors are overexpressed in the majority of human cancers, how tumor cells are sensitized to radiotherapies or chemotherapies upon integrin inhibition remains elusive. Here, we provide direct evidence in 3D lrECM cell culture models and in tumor xenografts that β_1 integrin targeting is a promising approach to sensitize tumor cells to radiotherapy and that the susceptibility of HNSCC cells to anti–β_1 integrin treatment depends on the activity of FAK. Further, to our knowledge, this study identified new regulatory motifs of FAK kinase activity and cortactin as a novel binding partner of FAK. Mechanistically, dissociation of cortactin from FAK, resulting in JNK1 deactivation, is a critical event leading to radiosensitization of tumor cells upon β_1 integrin inhibition.

Prior studies implicated that targeting integrins may be potentially useful to induce death of tumor cells or endothelial cells of the tumor vasculature and prevent neoangiogenesis (9, 47, 48). Additionally, tumor cell invasion and metastasis could be efficiently targeted, as these processes, at least partially, depend on integrins (49, 50). Compounds facilitating effective integrin inhibition include monoclonal antibodies like volociximab, synthetic peptides like cilengitide, and peptidomimetics, which are directed against different αβ integrin heterodimers or specific ECM-binding motifs on integrins (51, 52). Due to their expression on tumor cells and endothelium, a large body of preclinical and clinical work on $\alpha v\beta_3/\beta_5$ integrin inhibition indicates substantial tumor cell death in a variety of tumor entities, such as glioblastoma and lung cancer, in addition to providing imaging possibilities prior and during the course of therapy. Most importantly, all studies accomplished to date come to the same conclusion: monotherapeutic anti-integrin approaches are by far less efficient alone than in combination with chemotherapy and, particularly, radiotherapy, a strategy in line with modern multimodal treatment regimes (11, 22, 47).

Despite strong evidence for an enhancement of tumor cell chemosensitivity and radiosensitivity by β_1 integrin inhibition (8, 16, 21, 53), the underlying mechanisms are unclear. To address this issue, we chose the 3D lrECM based cell culture model and tumor xenografts in nude mice. Intriguingly, 8 out of 10 HNSCC cell lines exhibited susceptibility to antibody-mediated β_1 integrin inhibition. The same 8 cell lines showed enhanced radiosensitization in response to β_1 integrin inhibition, which was

confirmed by similar results from siRNA-mediated β_1 integrin knockdown. In a proof-of-principle study on tumors in vivo, we successfully demonstrated that a triple i.p. application of the inhibitory monoclonal anti–β_1 integrin antibody AIIB2 plus irradiation with 20 Gy significantly delayed the growth of UTSCC15 tumor xenografts. These promising results will now undergo further validation in preclinical translational studies using clinically relevant fractionated radiotherapy and permanent local tumor control as the end point. Interestingly, except for a reduction in the mitotic index, neither changes in BrdU, Ki-67, animal weight, or necrotic/hypoxic tumor areas nor increased metastasis were observable in AIIB2-treated mice.

To evaluate the responsible mechanisms and discriminate between responder and nonresponder HNSCC cell lines, a phosphoproteome array analysis was performed. Aside from specific modifications of cell proliferation-associated proteins, such as GSK3 and ERK2, we found strong downregulation of FAK phosphorylation. Further analysis revealed a deactivation of the FAK/paxillin/p130Cas signaling cascade by β_1 integrin inhibition in the responder cell lines UTSCC15 and XF354 and in UTSCC15 xenografts in contrast to the nonresponder cell line SAS. Although reduced phosphorylation of the FAK/paxillin/p130Cas protein complex is in line with results from many other studies (50, 54, 55), the reduced phosphorylation of JNK1 and JNK2 as well as absent Src modifications appear to be unique for HNSCC and particularly for 3D lrECM and in vivo growth conditions. Thus, signaling alterations induced by β_1 integrin inhibition seem to vary between tumor entities. For example, AIIB2 treatment of 3D lrECM–grown breast carcinoma cell lines mainly mediated deactivation of PI3K/Akt signaling (21), which was also found in lung carcinoma cells (55) but not in HNSCC as presented. Strong support for our hypothesis that FAK is most upstream to β_1 integrin signaling came from in situ PLAs, showing that the interaction between β_1 integrins and FAK is immediately released upon β_1 integrin blocking. Intriguingly, expression of either wild-type or constitutively active forms of FAK bypassed the effect of AIIB2 treatment and imparted significant radioprotection. Conclusively, these findings demonstrate that FAK is a key determinant of β_1 integrin downstream signaling, clonogenic cell survival, and radiosensitization by β_1 integrin inhibition of HNSCC cells.

Another obvious discrepancy between responder and nonresponder cells was cell rounding and FA disassembly upon AIIB2-mediated β_1 integrin blocking. To address this issue, we sought actin binding proteins in a complex with FAK. Mass spectrometry of FAK immunoprecipitates assisted us in identifying the actin organization regulators cortactin, cofilin, and ezrin/moesin. From this panel, only cortactin, a FAK-interacting protein, was unphosphorylated after AIIB2 treatment; this was associated with its dissociation from FAK, which remained until at least 24 hours. Further proof for FAK-cortactin binding as a key step downstream of β_1 integrin came from FAK, Src, JNK1, JNK2, or cortactin knockdown experiments and transfectants expressing the constitutively active kinase form of FAK that perpetuated FAK-cortactin binding upon AIIB2-mediated β_1 integrin inhibition.

To provide further evidence for a direct physical interaction between FAK and cortactin, to identify putative cortactin binding sequences on FAK, and to assess whether loss of cortactin binding to FAK impacts on radiosensitivity of 3D HNSCC cells, we mutated 2 PXΨP or 2 PXXPXXP motifs of FAK. These sequences function as SH3 consensus binding motifs for cortactin, as shown previously for cortactin and BPGAP1 (45). These motifs are located at very different regions of the FAK protein: the FERM and kinase domain linker domain, the kinase domain, the kinase-FAT linker domain, and the FAT domain. According to recent work on FAK activity regulation by cooperative FERM-kinase domain interactions (reviewed in ref. 46), we hypothesized that inactivating mutations at these motifs modify both FAK-cortactin binding and FAK phosphorylation and thus FAK activity. Indeed, mutations of the 2 PXΨP motifs located at the FERM-kinase domain linker and the FAT domain completely abrogated cortactin binding to FAK similar to the dominant-negative FRNK. The mutated PXXPXXP motif within the kinase domain led to strong reduction of this protein interaction. It can be speculated that both a sound regulatory interaction between the FERM and kinase domain and correct FAK targeting to FAs determine cortactin linkage to FAK. Importantly, these binding motifs represent essential regulatory sites for FAK activity that we believe to be novel. In contrast to the mutated PXXPXXP motif at the kinase domain-FAT linker, the other mutations caused pronounced dephosphorylation of FAK, cortactin, and JNK1. Strikingly, perturbation of FAK kinase activity and loss of FAK/cortactin interaction translated into significant enhancement of radiosensitivity. The lesser degree of radiosensitization as compared with that in controls and FRNK transfectants might be due to spatiotemporal patterns of specific fractions of FAK, cortactin, and the FAK/cortactin protein complex, which differentially govern additional functions of FAK and cortactin.

In summary, this study reveals mechanistic evidence for prosurvival and radioresistance-mediating signals via a β_1 integrin/FAK/cortactin/JNK1 pathway in HNSCC cells (Supplemental Figure 25). Moreover, these findings underscore β_1 integrin targeting as an attractive approach in combination with radiotherapy and radiochemotherapy for patients suffering from HNSCC. Consisting of a myriad of prosurvival signaling molecules, FA signaling hubs serve as major promoters of tumor growth and progression, whose specific targeting may be used to overcome therapy resistance for increasing cancer patient survival rates.

Methods

Cell cultures, 3D colony formation assay, radiation exposure, and antibody treatment. Human UTSCC45, UTSCC15, UTSCC14, UTSCC8, UTSCC5, SAS, Cal33, HSC4, XF354 HNSCC cell lines were provided by R. Grenman (Turku University Central Hospital, Turku, Finland). To evaluate 3D clonogenic cell survival, we imbedded cells in lrECM (Matrigel; BD), as previously published (23) and as described in the Supplemental Methods.

Antibodies. The following antibodies were used: anti–pFAK Y397 (for Western blotting), anti-FAK (for immunoprecipitation), anti–pSrc Y416, anti–pSrc Y529, anti-Src, anti–pcortactin Y421, anti-cortactin, anti-JNK, anti–pcofilin S3, anti-cofilin, anti-pezrin/radixin/moesin, anti-ezrin/radixin/moesin, anti–caspase-3, anti-ppaxillin Y118, anti-paxillin, and anti-pp130Cas Y410 (all from Cell Signaling Technology); anti-FAK (for Western blotting), anti–β_1 integrin, and anti-CD31 (all from BD); anti-p130Cas (Millipore); anti–β-actin (Sigma-Aldrich); anti-GFP (ab290; for Western blotting), anti-GFP (ab1218; for immunoprecipitation), and anti–pFAK Y397 (all from Abcam; for immunofluorescence); anti–Ki-67 and anti-BrdU (Dako); rabbit polyclonal anti-pimonidazole (provided by J. Raleigh, University of North Carolina, North Carolina, Chapel Hill, USA); HRP-conjugated donkey anti-rabbit and sheep anti-mouse secondary antibodies (GE Healthcare); and anti-FAK (for immunofluorescence),

anti–pJNK T183/Y185, and Alexa Fluor 594 goat anti-rabbit IgG (all from Invitrogen). The β_1 integrin inhibitory antibody, clone AIIB2, is a rat monoclonal IgG1 isolated from a human choriocarcinoma hybridoma. This antibody specifically binds to the extracellular domain of β_1 integrins (56). The β_1 integrin inhibitory antibody, clone 13, is a rat monoclonal IgG1 provided by K.M. Yamada (National Institute of Dental and Craniofacial Research, Bethesda, Maryland, USA). Different isotype control antibodies used were IgG#1 (rat; Santa Cruz Biotechnology Inc.), IgG#2 (rat; anti-ELAV; isolated from hybridoma cells, Developmental Studies Hybridoma Bank; see the Supplemental Methods), and IgG#3 (mouse; Santa Cruz Biotechnology Inc.).

Integrin analysis by flow cytometry. The β_1 integrin expression levels were measured by flow cytometry, as described previously (16) and as described in the Supplemental Methods.

Total protein extracts and Western blotting. Cells were harvested using modified RIPA buffer and subjected to SDS-PAGE and Western blotting, as previously described (23). For further information, see the Supplemental Methods.

Immunoprecipitation. Immunoprecipitation assays were performed as previously published (23). In brief, protein G-Agarose beads (Sigma-Aldrich) were incubated with specific antibodies overnight at 4°C. Beads were washed with 1x PBS, and 250 µl 3D lysates (Cell Lysis Buffer, Cell Signaling Technology) were added. After incubation overnight at 4°C, immunoprecipitates were washed, mixed with sample buffer, and loaded on SDS gels.

Mass spectrometric analysis. After immunoprecipitation, protein mixtures were separated on a gel and in-gel digested with trypsin, and peptides recovered from the gel matrix were analyzed on a LTQ Orbitrap XL mass spectrometer (Thermo Fisher Scientific) coupled online to the Ultima3000 LC system (Dionex) via a TriVersa robotic ion source (Advion BioScience), as recently published (23) and as described in the Supplemental Methods.

siRNA knockdown. β_1 Integrin, FAK, Src, JNK1, JNK2, and CTTN siRNA were purchased from Applied Biosystems. Negative control siRNA no. 1 (Applied Biosystems) was used as nonspecific control. siRNA delivery was accomplished as published previously (23). For further information, see the Supplemental Methods.

FAK expression constructs, FAK site-directed mutagenesis and transfection of FAK, and paxillin plasmids. Mouse FAKwt and FRNK fragments were generated by PCR-based amplification from expression plasmids provided by D.D. Schlaepfer (UCSD, San Diego, California, USA) and inserted into pEGFP-N1 (Clontech). The FAK activation loop and putative cortactin binding sites were mutated using QuikChange II Site-Directed Mutagenesis Kit (Stratagene) according to manufacturer's instructions. Paxillin-GFP plasmid was a gift from A.R. Horwitz (University of Virginia, Charlottesville, Virginia USA). Cells were stably transfected with FAK and paxillin plasmids, as published previously (23). For more detailed information, see the Supplemental Methods.

Kinetworks phosphoprotein analysis. Cells were harvested by scraping into lysis buffer, as described previously (57), according to the manufacturer's instructions. For phosphorylation analysis, KPSS-1.3 and KPSS-11.0 phospho-site screens were performed, and, for total protein expression, KPKS-1.2 protein kinase screens were performed. For further information, see the Supplemental Methods.

PLA. Proximity ligation was performed according to the manufacturer's protocol using the Duolink Detection Kit with PLA PLUS and MINUS Probes for mouse and rabbit (Olink Bioscience; ref. 43). Samples were analyzed with a confocal microscope (LSM 510 Meta; Carl Zeiss Inc.) under a ×63 oil objective. For more detailed information, see the Supplemental Methods.

Sequence homology search. The sequence homology search for the PXΨP and PXXPXXP motifs in the FAK protein sequence was performed (*Homo sapiens*, accession no. NP_722560; *Mus musculus*, accession no. NP_032008; *Rattus norvegicus*, accession no. NP_037213; *Gallus gallus*, accession no. NP_990766; *Xenopus laevis*, accession no. NP_001084066) using MultAlin (http://bioinfo.genotoul.fr/multalin/multalin.html) and ESPript 2.2 (http://espript.ibcp.fr/ESPript/ESPript/index.php).

Mice and in vivo experiments. Animal facilities and experiments were approved by the Regierungsministerium Dresden (Dresden, Germany), according to the German and Saxony animal welfare regulations. Immunocompromised 7- to 14-week-old male and female NMRI (*nu/nu*) mice (Experimental Centre of the Medical Faculty Carl Gustav Carus; Technische Universität Dresden) were further immunosuppressed by whole body irradiation 1–5 days before subcutaneous tumor transplantation onto the right hind leg. After reaching a tumor volume of approximately 100 mm^3, animals were randomly allocated to the different treatment arms. The tumor diameter was measured twice per week using a caliper (5, 23). Tumor growth time (GT) was evaluated from growth curves of individual tumors as the time needed after the start of the experiment to reach 2 and 5 times the starting volume (GT_{V2} and GT_{V5}). Medians and SEMs were calculated for each treatment group, and comparisons were performed by the Mann-Whitney *U* test. Animals were followed up until tumors reached a volume of about 1.5 cm^3 or until death of the animal. For ex vivo investigations of the tumors, animals were treated in parallel to the growth delay experiments. Tumors were fixed overnight in 4% formalin and embedded in paraffin, and labeling indices for BrdU and Ki-67 were obtained from 10 randomly chosen viewing fields per tumor section according to standard procedures. Further, evaluation of the hypoxic, necrotic, and vital tumor areas was performed from 10 randomly chosen viewing fields per tumor section. All samples were blinded for analysis. For further information, see the Supplemental Methods.

Statistics. Data are presented as mean ± SD or mean ± SEM. The level of significance was determined by unpaired, 2-tailed Student's *t* test and Mann-Whitney *U* test (median values for tumor growth time) (GraphPad Prism software 4.03). Results were considered statistically significant if a *P* value of less than 0.05 was reached.

Study approval. All animal experiments have been approved by the Regierungsministerium Dresden (Dresden, Germany), according to the German and Saxony animal welfare regulations.

Acknowledgments

We thank R. Grenman, A.R. Horwitz, J. Raleigh, D.D. Schlaepfer, and K.M. Yamada for reagents; L. Kunz-Schughart for cell sorting; and I. Lange and K. Schumann for excellent technical assistance. We are grateful to R. Fässler, K. Legate, and A. Vehlow for critically reading the manuscript. This work was funded in part by the Bundesministerium für Bildung und Forschung 03ZIK041, the Saxon Ministry of Science and Arts 100066308 (to M. Baumann and N. Cordes), the Deutsche Krebshilfe e.V. 108976 (to N. Cordes), the Deutsche Forschungsgemeinschaft Ba1433/5 (to M. Baumann and M. Krause), and the Medical Faculty Carl Gustav Carus, Dresden University of Technology, Germany (MeDDrive grant to I. Eke). All authors discussed the results, commented on the manuscript, and approved the final manuscript.

Received for publication October 6, 2011, and accepted in revised form January 18, 2012.

Address correspondence to: Nils Cordes, OncoRay – National Center for Radiation Research in Oncology, Medical Faculty Carl Gustav Carus, Dresden University of Technology, Fetscherstrasse 74 / PF 41, 01307 Dresden, Germany. Phone: 49.0.351.458.7401; Fax: 49.0.351.458.7311; E-mail: Nils.Cordes@OncoRay.de.

1. Baumann M, Krause M, Hill R. Exploring the role of cancer stem cells in radioresistance. *Nat Rev Cancer*. 2008;8(7):545–554.
2. Hanahan D, Weinberg RA. Hallmarks of cancer: the next generation. *Cell*. 2010;144(5):646–674.
3. Karnoub AE, Weinberg RA. Ras oncogenes: split personalities. *Nat Rev Mol Cell Biol*. 2008;9(7):517–531.
4. Gerber DE, Minna JD. ALK inhibition for non-small cell lung cancer: from discovery to therapy in record time. *Cancer Cell*. 2011;18(6):548–551.
5. Krause M, Gurtner K, Deuse Y, Baumann M. Heterogeneity of tumour response to combined radiotherapy and EGFR inhibitors: differences between antibodies and TK inhibitors. *Int J Radiat Biol*. 2009; 85(11):943–954.
6. Sawyers C. Targeted cancer therapy. *Nature*. 2004; 432(7015):294–297.
7. Bonner JA, et al. Radiotherapy plus cetuximab for squamous-cell carcinoma of the head and neck. *N Engl J Med*. 2006;354(6):567–578.
8. Damiano JS. Integrins as novel drug targets for overcoming innate drug resistance. *Curr Cancer Drug Targets*. 2002;2(1):37–43.
9. Desgrosellier JS, Cheresh DA. Integrins in cancer: biological implications and therapeutic opportunities. *Nat Rev Cancer*. 2010;10(1):9–22.
10. Hehlgans S, Haase M, Cordes N. Signalling via integrins: implications for cell survival and anticancer strategies. *Biochim Biophys Acta*. 2007; 1775(1):163–180.
11. Ruegg C, Alghisi GC. Vascular integrins: therapeutic and imaging targets of tumor angiogenesis. *Recent Results Cancer Res*. 2010;180:83–101.
12. Weaver VM, et al. beta4 integrin-dependent formation of polarized three-dimensional architecture confers resistance to apoptosis in normal and malignant mammary epithelium. *Cancer Cell*. 2002; 2(3):205–216.
13. Eriksen JG, Steiniche T, Sogaard H, Overgaard J. Expression of integrins and E-cadherin in squamous cell carcinomas of the head and neck. *Apmis*. 2004; 112(9):560–568.
14. Yao ES, et al. Increased beta1 integrin is associated with decreased survival in invasive breast cancer. *Cancer Res*. 2007;67(2):659–664.
15. Janes SM, Watt FM. New roles for integrins in squamous-cell carcinoma. *Nat Rev Cancer*. 2006; 6(3):175–183.
16. Cordes N, Seidler J, Durzok R, Geinitz H, Brakebusch C. beta1-integrin-mediated signaling essentially contributes to cell survival after radiation-induced genotoxic injury. *Oncogene*. 2006; 25(9):1378–1390.
17. Hynes RO. Integrins: bidirectional, allosteric signaling machines. *Cell*. 2002;110(6):673–687.
18. Moser M, Legate KR, Zent R, Fassler R. The tail of integrins, talin, and kindlins. *Science*. 2009; 324(5929):895–899.
19. Shibue T, Weinberg RA. Integrin beta1-focal adhesion kinase signaling directs the proliferation of metastatic cancer cells disseminated in the lungs. *Proc Natl Acad Sci U S A*. 2009;106(25):10290–10295.
20. Ramirez NE, et al. The alphabeta integrin is a metastasis suppressor in mouse models and human cancer. *J Clin Invest*. 2010;121(1):226–237.
21. Park CC, Zhang HJ, Yao ES, Park CJ, Bissell MJ. Beta1 integrin inhibition dramatically enhances radiotherapy efficacy in human breast cancer xenografts. *Cancer Res*. 2008;68(11):4398–4405.
22. Meads MB, Gatenby RA, Dalton WS. Environment-mediated drug resistance: a major contributor to minimal residual disease. *Nat Rev Cancer*. 2009; 9(9):665–674.
23. Eke I, et al. PINCH1 regulates Akt1 activation and enhances radioresistance by inhibiting PP1alpha. *J Clin Invest*. 2010;120(7):2516–2527.
24. Legate KR, Fassler R. Mechanisms that regulate adaptor binding to beta-integrin cytoplasmic tails. *J Cell Sci*. 2009;122(pt 2):187–198.
25. Kasahara T, Koguchi E, Funakoshi M, Aizu-Yokota E, Sonoda Y. Antiapoptotic action of focal adhesion kinase (FAK) against ionizing radiation. *Antioxid Redox Signal*. 2002;4(3):491–499.
26. Lim ST, Mikolon D, Stupack DG, Schlaepfer DD. FERM control of FAK function: implications for cancer therapy. *Cell Cycle*. 2008;7(15):2306–2314.
27. Sood AK, et al. Adrenergic modulation of focal adhesion kinase protects human ovarian cancer cells from anoikis. *J Clin Invest*. 2010;120(5):1515–1523.
28. Yuan Z, Zheng Q, Fan J, Ai KX, Chen J, Huang XY. Expression and prognostic significance of focal adhesion kinase in hepatocellular carcinoma. *J Cancer Res Clin Oncol*. 2010;136(10):1489–1496.
29. Cance WG, et al. Immunohistochemical analyses of focal adhesion kinase expression in benign and malignant human breast and colon tissues: correlation with preinvasive and invasive phenotypes. *Clin Cancer Res*. 2000;6(6):2417–2423.
30. Owens LV, et al. Overexpression of the focal adhesion kinase (p125FAK) in invasive human tumors. *Cancer Res*. 1995;55(13):2752–2755.
31. Schaller MD, Hildebrand JD, Shannon JD, Fox JW, Vines RR, Parsons JT. Autophosphorylation of the focal adhesion kinase, pp125FAK, directs SH2-dependent binding of pp60src. *Mol Cell Biol*. 1994; 14(3):1680–1688.
32. Huang C, Jacobson K, Schaller MD. MAP kinases and cell migration. *J Cell Sci*. 2004;117(pt 20):4619–4628.
33. Ng J, Luo L. Rho GTPases regulate axon growth through convergent and divergent signaling pathways. *Neuron*. 2004;44(5):779–793.
34. Liu S, Calderwood DA, Ginsberg MH. Integrin cytoplasmic domain-binding proteins. *J Cell Sci*. 2000; 113(pt 20):3563–3571.
35. Higgs HN, Pollard TD. Regulation of actin filament network formation through ARP2/3 complex: activation by a diverse array of proteins. *Annu Rev Biochem*. 2001;70:649–676.
36. Weed SA, Parsons JT. Cortactin: coupling membrane dynamics to cortical actin assembly. *Oncogene*. 2001;20(44):6418–6434.
37. Clark ES, Whigham AS, Yarbrough WG, Weaver AM. Cortactin is an essential regulator of matrix metalloproteinase secretion and extracellular matrix degradation in invadopodia. *Cancer Res*. 2007; 67(9):4227–4235.
38. Shibata T, Kokubu A, Sekine S, Kanai Y, Hirohashi S. Cytoplasmic p120ctn regulates the invasive phenotypes of E-cadherin-deficient breast cancer. *Am J Pathol*. 2004;164(6):2269–2278.
39. Schubert V, Dotti CG. Transmitting on actin: synaptic control of dendritic architecture. *J Cell Sci*. 2007; 120(pt 2):205–212.
40. Webb BA, Jia L, Eves R, Mak AS. Dissecting the functional domain requirements of cortactin in invadopodia formation. *Eur J Cell Biol*. 2007; 86(4):189–206.
41. Ridley AJ, Hall A. The small GTP-binding protein rho regulates the assembly of focal adhesions and actin stress fibers in response to growth factors. *Cell*. 1992;70(3):389–399.
42. Serrels B, et al. Focal adhesion kinase controls actin assembly via a FERM-mediated interaction with the Arp2/3 complex. *Nat Cell Biol*. 2007;9(9):1046–1056.
43. Jarvius J, et al. Digital quantification using amplified single-molecule detection. *Nat Methods*. 2006; 3(9):725–727.
44. Gabarra-Niecko V, Keely PJ, Schaller MD. Characterization of an activated mutant of focal adhesion kinase: 'SuperFAK'. *Biochem J*. 2002; 365(pt 3):591–603.
45. Lua BL, Low BC. BPGAP1 interacts with cortactin and facilitates its translocation to cell periphery for enhanced cell migration. *Mol Biol Cell*. 2004; 15(6):2873–2883.
46. Frame MC, Patel H, Serrels B, Lietha D, Eck MJ. The FERM domain: organizing the structure and function of FAK. *Nat Rev Mol Cell Biol*. 2010;11(11):802–814.
47. Cordes N, Park CC. beta1 integrin as a molecular therapeutic target. *Int J Radiat Biol*. 2007; 83(11–12):753–760.
48. Sugahara KN, et al. Tissue-penetrating delivery of compounds and nanoparticles into tumors. *Cancer Cell*. 2009;16(6):510–520.
49. Friedl P, Gilmour D. Collective cell migration in morphogenesis, regeneration and cancer. *Nat Rev Mol Cell Biol*. 2009;10(7):445–457.
50. Kim SA, Kwon SM, Kim JA, Kang KW, Yoon JH, Ahn SG. 5′-Nitro-indirubinoxime, an indirubin derivative, suppresses metastatic ability of human head and neck cancer cells through the inhibition of Integrin beta1/FAK/Akt signaling. *Cancer Lett*. 2011; 306(2):197–204.
51. Mas-Moruno C, Rechenmacher F, Kessler H. Cilengitide: the first anti-angiogenic small molecule drug candidate design, synthesis and clinical evaluation. *Anticancer Agents Med Chem*. 2010;10(10):753–768.
52. Ricart AD, et al. Volociximab, a chimeric monoclonal antibody that specifically binds alpha5beta1 integrin: a phase I, pharmacokinetic, and biological correlative study. *Clin Cancer Res*. 2008;14(23):7924–7929.
53. Estrugo D, Fischer A, Hess F, Scherthan H, Belka C, Cordes N. Ligand bound beta1 integrins inhibit procaspase-8 for mediating cell adhesion-mediated drug and radiation resistance in human leukemia cells. *PLoS One*. 2007;2(3):e269.
54. Mitra SK, Hanson DA, Schlaepfer DD. Focal adhesion kinase: in command and control of cell motility. *Nat Rev Mol Cell Biol*. 2005;6(1):56–68.
55. Morello V, et al. β1 integrin controls EGFR signaling and tumorigenic properties of lung cancer cells. *Oncogene*. 2011;30(39):4087–4096.
56. Werb Z, Tremble PM, Behrendtsen O, Crowley E, Damsky CH. Signal transduction through the fibronectin receptor induces collagenase and stromelysin gene expression. *J Cell Biol*. 1989; 109(2):877–889.
57. Zhang H, Shi X, Paddon H, Hampong M, Dai W, Pelech S. B23/nucleophosmin serine 4 phosphorylation mediates mitotic functions of polo-like kinase 1. *J Biol Chem*. 2004;279(34):35726–35734.